Earthq Eng & Eng Vib (2020) 19: 189-204 **DOI**: https://doi.org/10.1007/s11803-020-0556-z

Availability of seismic vulnerability index (K_g) in the assessment of building damage in Van, Eastern Turkey

İsmail Akkaya†

Van Yüzüncü Yıl University, Engineering Faculty, Department of Geophysical Engineering, Van 65080, Turkey

Abstract: The seismic vulnerability index (K_g) is a parameter that depends on the dynamic properties of soil. With this parameter, it is possible to evaluate the vulnerability of a point-based site under strong ground motion. Since it is related to the natural vibration period and amplification factor, the parameter can be calculated for both soil and structure. In this study, HVSR microtremor measurements are recorded at more than 200 points in the Van region to generate a seismic vulnerability index map. After generating the map, it is determined that the hazard potential and seismic vulnerability index is high at the sites close to Van Lake and at the densely populated city center. Damage information of the buildings investigated after the 2011 Van earthquakes (M_w = 7.1) are placed on the seismic vulnerability index map and it is realized that there may be a correlation between the damage and the seismic vulnerability index. There is a high correlation, approximately 80 percent, between the damage rate map based on the damaged building data and the K_g values. In addition, vulnerability indexes of buildings are calculated and the effect of local soil conditions and building properties on the damage levels are determined. From the results of this study and the site observations after the 2011 Van earthquakes, it is found that structural damage is not only structure-dependent but is also related to the dynamic behavior of soil layers and local soil conditions.

Keywords: seismic vulnerability index; building damage; HVSR; soil-structure interaction

1 Introduction

Van settlements (Eastern Turkey) and its surrounding areas have affected very complex tectonic processes in geological time. The Lake Van region has a high level of seismicity, both historical (before 1900) and more recently as recorded by instrumental period (Koçyiğit *et al*., 2001; Akkaya, 2015; Akkaya *et al*., 2015). Local soil conditions, earthquake characteristics and structural properties are the main factors causing distribution of structural damage at the time of the earthquakes and have an important role in the soil-structure interaction (Ansal, 1999a, b). Poor construction practices and local site effects play a crucial role in determining earthquake hazards of these regions. The level of building damage during an earthquake is closely related to the softness and thickness of the sediment layers.

The HVSR microtremor method, which is the best approach to predict the site effects due to seismic wave propagation, is commonly used to determine the damage caused by destructive earthquakes (Nakamura, 1997, 2000, 2008). The single-station microtremor measurements technique, known as the H/V spectral ratio (HVSR) method developed by Nakamura (1989), is one of the easiest and most reliable methods for determining local soil conditions. Amplification factor and predominant frequency of the soil are HVSR parameters, which are related to the local soil conditions and soil-structure interaction. HVSR were used to determine the amplification (HVSR peak value), predominant period and seismic vulnerability index (K_g) values also affected by the geotechnical conditions, soil type, and thickness of the sediment layer. The method has been commonly used in engineering applications by many researchers to analyze site effects and earthquake ground motion amplification (Nakamura, 1989, 1997, 2000; Field and Jacob, 1993, 1995; Lachet and Bard, 1994; Bard, 1998; Lermo and Chavez-Garcia, 1993,1994; Konno and Ohmachi, 1998; SESAME, 2004; Gallipoli and Mucciarelli, 2009; Paudyal *et al*., 2012; Akkaya, 2015; Akkaya *et al*., 2015, Livaoğlu *et al*., 2017; Pamuk *et al*., 2017a-c; Akkaya and Özvan, 2019).

Microtremor applications are used to evaluate the K_g value. The K_g value may also be useful as an indicator of the weak points in a region. In addition, K_g has an important role in earthquake hazards studies. K_g depends on the dominant frequency, HVSR amplification factor and V_{s30} value of the soil (Nakamura, 1997). Recently, K_g

Correspondence to: İsmail Akkaya, Department of Geophysical Engineering, Engineering Faculty, Van Yüzüncü Yıl University, Van 65080, Turkey
Tel: +90-533 550 7428; Fax: +90-432 225 1732
E-mail: iakkaya@yyu.edu.tr
†PhD

Supported by: Scientific Research Projects Office of Van Yüzüncü Yıl University Project Number 2015-MIM-B259
Received July 25, 2018; **Accepted** November 15, 2018

has been used by many researchers in the distribution of damage and in microzonation studies (Nakamura, 1997, 2000, 2008; Gallipoli *et al*., 2004; Nath *et al*., 2015; Dindar *et al*., 2017; Livaoğlu *et al*., 2017; Pamuk *et al*., 2017a-c).

The Van earthquake occurred on October 23, 2011, and struck the region (Eastern Turkey) with a moment magnitude of 7.1, resulting in the deaths of 644 people (KOERI, 2011). After the earthquake, 36 buildings totally collapsed, 20,547 buildings sustained heavy damage, 6,607 buildings were moderately damaged and 59,796 buildings suffered only light damage (documented by AFAD) used as the study area to understand the relationship between building damage and the K_g value.

In this study, HVSR microtremor data measurements were performed at more than 200 sites in order to identify the soil properties, amplification factor, and predominant frequency or period values in the Van settlement area (Fig. 1). HVSR data were analyzed using the Nakamura method. The K_g value was evaluated using the HVSR amplification factor and predominant frequency or period, which was used to determine the earthquake hazards on the site. In order to investigate the engineering properties of the study area and the K_g, amplification, predominant period, shear wave V_{s30} velocity, soil classification, and building damage ratio, maps have been prepared.

2 Geology and seismicity of the region

The study area is located in the eastern sites of the Lake Van region in Eastern Turkey (Fig. 1). The Lake Van region lies along the continental collision zone between the Eurasian and Arabian plates, and consists of different types of rock units and alluvium. The Lake Van

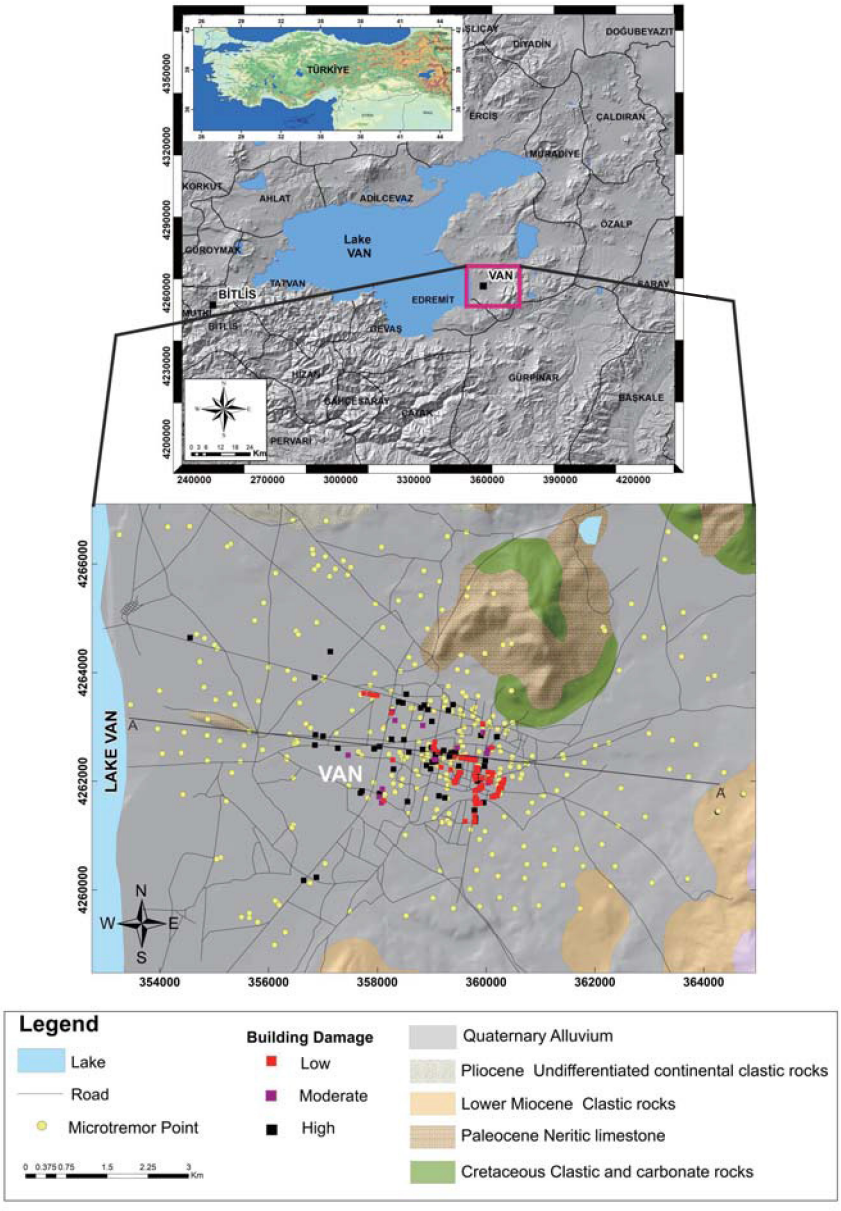

Fig. 1 Location and measurement point map of the study area

basin consists of three major geological units: Paleozoic metamorphic rocks and Upper Cretaceous ophiolites, volcanic rocks, and Miocene and Quaternary alluvium (Fig. 1). The predominant geological units in the eastern site of the region consist of Miocene and Quaternary age alluvial deposits and lake sediments. A large part of the studied area is located over a ground composed of the recent alluvium. These deposits include silt, sand, gravels, and loose and soft clay. Sedimentation processes in the area are due to oscillations in the lake water level over time. The level of groundwater is shallow particularly in the nearest of Lake Van, as shown by the borehole data. In general, the level of groundwater observed was less than 20 m in the region, particularly in old lake sediments. The level of groundwater especially decreased (< 5 m) in the nearest parts of Lake Van, in the recent alluvial deposits (Özvan *et al*., 2005; Akkaya *et al*., 2015, 2017, 2018a).

The continental collision between the Eurasian and the Arabian plates in Late Miocene caused crustal shortening, thickening and uplift of the Eastern Anatolian region (Şengör and Kidd, 1979; Şaroğlu and Yılmaz, 1986; Koçyiğit *et al*., 2001). Because of this collision, the Anatolian Plate escaped in a westward direction along the East and North Anatolian fault zones (Şaroğlu and Yılmaz, 1986). In addition, this collision caused the formation of the Lake Van basin. The region is under the influence of the north–south directional compression regime. After the collision, many *NW* trending strike-slip, *E–W* trending reverse or thrust, and normal faults were developed (Bozkurt, 2001; Koçyiğit *et al*., 2001; Koçyiğit, 2013).

The Lake Van area is situated in the most seismically active region in Turkey and is subjected to tectonic movement. Strike-slip and thrust faults are the major tectonic units in the region, such as the Van thrust fault, Çaldıran, Gürpınar and Erciş–Kocapınar fault zone, Alaköy, Çolpan, Everek, and Özalp fault (Koçyiğit, 2013; Utkucu, 2013; Selçuk, 2016; Toker *et al*., 2017). Numerous destructive earthquakes have occurred both throughout history and in recent times around the Lake Van area, such as the 1111 Van, 1646 Hayatsdzaron, 1715 Hoşap, 1945 Van (M_s = 5.8), 1941 Erciş (M_s = 5.9), 1966 Varto (M_s = 6.8), 1903 Malazgirt (M_s = 6.3), 1976 Çaldıran (M_s = 7.5), and 2011 Van (M_w = 7.1; 5.6) earthquakes (Ambraseys and Finkel, 1995; Soysal *et al*., 1981; Ambraseys, 2001; Tan *et al*., 2008; Koçyiğit, 2013). In addition, earthquakes having $M \geq 5$ have been recorded during historical and instrumental periods in the Lake Van basin (Fig. 2). The Çaldıran, Van, and Erciş–Kocapınar Fault are very active fault zones that can adversely affect the region. There have been more than 15,000 earthquakes in the Lake Van region since 1900 (Fig. 2). The magnitude and depth diagrams of these earthquakes are shown in Fig. 2.

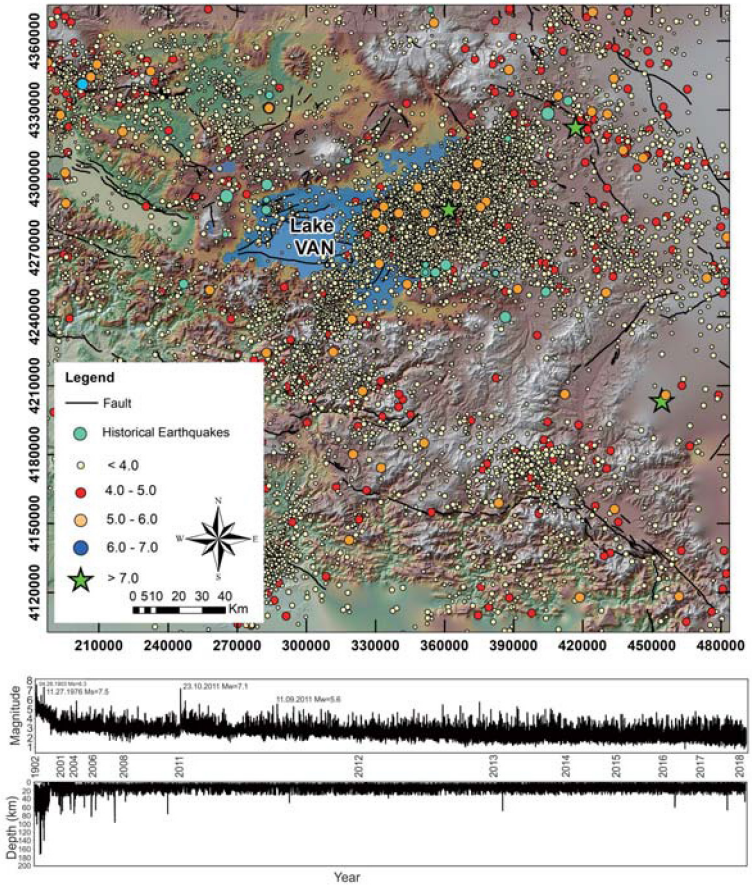

Fig. 2 Seismotectonic map of the region (the faults modified from Emre *et al*., 2013; Cukur *et al*., 2016)

3 HVSR microtremor measurements and data analysis

The HVSR microtremor technique, well known as the H/V or Nakamura (1989) method, is widely used for earthquake engineering applications. Nakamura (1989) showed that the predominant frequency or period and HVSR peak value or amplification factor of the soil site was related to the ratio of H/V components ambient noise records. The aim of the technique is to determine the HVSR peak value (amplitude) and peak frequencies/periods values based on ambient noise record. Local soil conditions and soil–structure interactions are related to the HVSR parameters. In the last century, the HVSR method has been tested and used by different researchers at many sites (Nakamura, 1989, 2000; Field and Jacob, 1993,1995; Lachet and Bard, 1994; Lermo and Chavez-Garcia, 1993, 1994; Gitterman *et al*., 1996; Konno and Ohmachi, 1998; Bard, 1998; Mucciarelli, 1998; Theodulidis *et al*., 1996; Delgado *et al*., 2000; Fah *et al*., 2001; Okada, 2003; Bonnefoy-Claudet *et al*., 2006; Dikmen and Mirzaoğlu, 2005; Birgoren *et al*., 2009; Özalaybey *et al*., 2011; Claprood *et al*., 2012; Eskişar *et al*., 2013; Akkaya, 2015; Akkaya *et al*., 2015; Silahtar *et al*., 2016; Akın and Sayıl, 2016; Tün *et al*., 2016; Pamuk *et al*., 2017a, b; Livaoğlu *et al*., 2017; Akkaya and Özvan, 2019).

According to the HVSR method, microtremor measurements were performed at more than 200 different sites in order to identify the soil properties and seismic vulnerability in the Van settlement area during 2016–2017 (Fig. 1). The HVSR data were recorded for 100 Hz sampling rate and a 30-minute recording duration at each site. The measurements were taken during the early hours of the day and night, especially in the city centers because of the heavy traffic throughout the day. In addition, data were recorded in convenient environmental conditions without rain and wind. HVSR data were taken with a CMG-6TD series Guralp Systems broadband velocity seismometer system. Measurements were visualized using the version 4.5 of Scream software. All data signals processing stage to remove intensive artificial disturbance by bandpass filtering of the full wave form with a band-pass of 0.01–20 Hz. After this step, the data were divided into 20–30 second window lengths, using cosine taper individually and the Konno & Ohmachi (1998) smoothing method with a constant number of 40. A fast fourier transform (FFT) was applied to obtain the amplitude spectra of the two horizontal (*NS* and *EW*) and one vertical (*Z*) components for each window. Finally, the average spectral ratio of the components was calculated (Fig. 3, Table 1). The open-source Geopsy software packages (GEOPSY, 1997), prepared by the recommendations of the SESAME (2004) Project, and was used in the data processing. As a result, the data was processed to obtain a distribution map of the predominant period and amplification factor in the study area (Fig. 4). The position of east-west directional depth section (*AA′*) is shown in Fig. 1.

Depth cross-section was created for the study area, taking into account the vertical and horizontal soil variations observed in the borehole (the maximum drilled depth approximately 5 km) and seismic data (Fig. 3). The HVSR microtremor measurement results for the same profile are given in Fig. 3, in which the bold line is the average HVSR value of the FFT analysis. The resulting spectra include the standard deviation for all values, which is represented by two dotted lines above and below. It was determined that there is a good correlation between the soil type and HVSR microtremor results in the cross-section created in the east-west direction in the study area (Fig. 3). Because of this profile, low amplitude and high frequency values were observed in the rocks and solid soil layers, whereas high amplitude and low–medium frequency values are observed in the case of weak soils. In the center of the

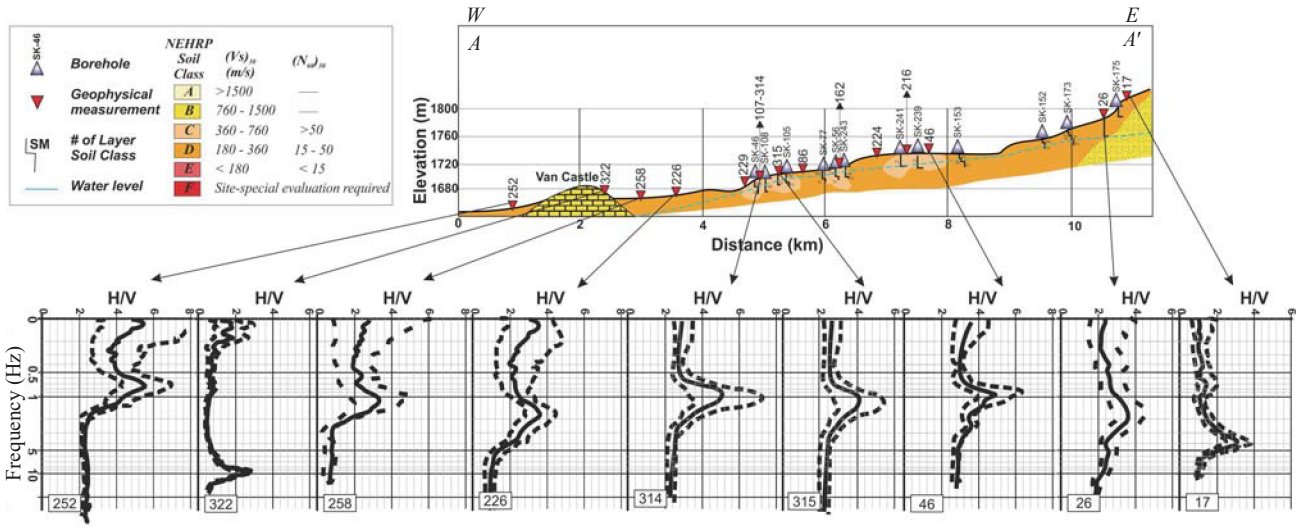

Fig. 3 East-West direction cross-section and HVSR microtremor results

Table 1 Measurement and calculated parameters used in this study

No.	Measurements name	Latitude X	Longitude Y	V_{s30} (m/s)	Soil class	H/V peak amplitude	f_0 (Hz)	t_0 (s)	K_g value
1	S + HV1	354874	4268327	1050	B	1.20	5.00	0.20	0.29
2	S + HV2	354859	4268319	946	B	1.20	5.00	0.20	0.29
3	S + HV6	355755	4268354	652	C	1.50	3.33	0.30	0.68
4	S + HV7	355615	4268957	584	C	1.50	3.33	0.30	0.68
5	S + HV12	359040	4263298	347	D	2.70	1.67	0.60	4.37
6	S + HV14	359861	4262301	301	D	4.11	1.59	0.63	10.64
7	S + HV16	355561	4267256	674	C	1.50	6.67	0.15	0.34
8	S + HV17	364805	4262270	550	C	2.45	3.33	0.30	1.80
9	S + HV19	359152	4260347	557	C	2.00	3.03	0.33	1.32
10	S + HV21	357859	4262905	237	D	3.45	2.50	0.40	4.76
11	S + HV26	363722	4262082	347	D	3.20	1.82	0.55	5.63
12	S + HV28	358921	4264811	251	D	3.67	3.23	0.31	4.18
13	S + HV29	359191	4265156	235	D	3.51	3.13	0.32	3.94
14	S + HV32	360216	4260256	344	D	2.50	3.23	0.31	1.94
15	S + HV35	360694	4260802	293	D	2.80	2.50	0.40	3.14
16	S + HV38	360629	4262051	274	D	3.25	2.70	0.37	3.91
17	S + HV39	360213	4261919	245	D	3.62	2.50	0.40	5.24
18	S + HV42	359285	4266509	285	D	3.11	2.86	0.35	3.39
19	S + HV45	359702	4260397	371	C	4.84	1.23	0.81	18.97
20	S + HV46	361520	4262240	362	C	4.62	0.79	1.27	27.11
21	S49	354698	4267928	1255	B	1.00	3.33	0.30	0.30
22	S86	359350	4262313	331	D	2.60	1.67	0.60	4.06
23	S118	355297	4268285	751	C	1.80	7.14	0.14	0.45
24	S126	355674	4269013	1060	B	1.40	5.00	0.20	0.39
25	M+ HV55	358903	4263388	442	C	2.12	3.33	0.30	1.35
26	M+ HV59	359246	4263376	285	D	2.30	1.43	0.70	3.70
27	M+ HV61	359005	4262287	232	D	2.84	1.11	0.90	7.26
28	M+ HV69	360331	4261348	230	D	3.41	1.96	0.51	5.93
29	M+ HV70	359628	4263563	332	D	2.30	1.67	0.60	3.17
30	M+ HV72	358270	4263332	273	D	2.75	2.33	0.43	3.25
31	M+ HV77	360048	4262070	323	D	3.96	1.67	0.60	9.41
32	M+ HV78	355745	4264958	250	D	2.50	1.25	0.80	5.00
33	M+ HV79	360441	4262267	376	C	4.20	2.33	0.43	7.59
34	M+ HV80	357966	4265265	295	D	2.83	1.43	0.70	5.61
35	M+ HV83	359968	4262877	262	D	2.95	2.33	0.43	3.74
36	M+ HV86	358481	4263010	352	D	3.24	1.64	0.61	6.40
37	M+ HV89	356444	4262824	291	D	3.67	2.00	0.50	6.73
38	M+ HV92	358212	4262499	315	D	3.16	1.54	0.65	6.49
39	M+ HV93	361022	4261737	211	D	3.83	1.43	0.70	10.27
40	M+ HV95	359484	4262571	292	D	2.86	1.43	0.70	5.73
41	M+ HV97	355294	4267660	492	C	1.80	2.50	0.40	1.30
42	M+ HV100	354738	4268704	434	C	2.30	2.50	0.40	2.12
43	M+ HV101	360340	4263067	335	D	2.66	2.00	0.50	3.54
44	HV107	354876	4262374	-	-	8.14	0.68	1.48	98.06
45	HV108	359090	4264498	-	-	2.10	5.00	0.20	0.88
46	HV109	359975	4264353	-	-	2.50	5.00	0.20	1.25
47	HV110	356306	4259220	-	-	2.50	2.00	0.50	3.13
48	HV111	363590	4264297	-	-	2.50	2.00	0.50	3.13
49	HV112	353994	4263664	-	-	3.00	1.43	0.70	6.30
50	HV113	361727	4259659	-	-	1.50	5.00	0.20	0.45
51	HV114	362903	4264652	-	-	2.70	2.00	0.50	3.65
52	HV115	354448	4262899	-	-	5.50	0.75	1.34	40.54
53	HV116	355769	4262616	-	-	3.00	1.43	0.70	6.30
54	HV117	353829	4264044	-	-	8.80	0.44	2.27	176.00
55	HV118	354435	4264134	-	-	8.70	0.61	1.64	124.08
56	HV119	355074	4264047	-	-	3.54	0.67	1.49	18.70
57	HV120	355575	4263968	-	-	5.75	0.60	1.66	54.88
58	HV121	356040	4262889	-	-	3.23	1.53	0.65	6.82
59	HV122	356904	4262901	-	-	4.21	0.67	1.49	26.45
60	HV123	358021	4262841	-	-	3.20	1.72	0.58	5.95

Table 1 Continued

No.	Measurements name	Latitude X	Longitude Y	V_{s30} (m/s)	Soil class	H/V peak amplitude	f_0 (Hz)	t_0 (s)	K_g value
61	HV124	358649	4262644	-	-	2.73	1.46	0.68	5.10
62	HV125	358056	4262291	-	-	3.84	1.44	0.69	10.24
63	HV126	358742	4261932	-	-	2.56	0.62	1.61	10.57
64	HV127	359160	4261484	-	-	3.70	0.68	1.47	20.13
65	HV128	359062	4263151	-	-	2.89	0.65	1.54	12.85
66	HV129	353370	4265125	-	-	1.89	0.64	1.56	5.58
67	HV130	354487	4264857	-	-	3.36	0.52	1.92	21.71
68	HV131	354415	4265100	-	-	3.93	0.55	1.82	28.08
69	HV132	355442	4264542	-	-	7.30	0.60	1.67	88.82
70	HV133	356039	4264066	-	-	3.80	0.65	1.54	22.22
71	HV134	356941	4263921	-	-	2.61	0.62	1.61	10.99
72	HV135	356968	4263669	-	-	3.25	0.80	1.25	13.20
73	HV136	358092	4263602	-	-	7.20	0.67	1.49	77.37
74	HV137	358443	4263572	-	-	3.75	0.68	1.47	20.68
75	HV138	358474	4263184	-	-	3.12	0.60	1.67	16.22
76	HV139	358577	4262863	-	-	2.81	1.51	0.66	5.23
77	HV140	358833	4262823	-	-	3.02	0.60	1.67	15.20
78	HV141	359357	4263054	-	-	3.58	0.60	1.67	21.36
79	HV142	359654	4263479	-	-	2.10	0.60	1.67	7.35
80	HV143	359472	4263466	-	-	2.83	0.51	1.96	15.70
81	HV144	359097	4263534	-	-	2.29	1.51	0.66	3.47
82	HV145	359087	4263534	-	-	2.18	1.46	0.68	3.26
83	HV146	360598	4262906	-	-	2.55	0.63	1.59	10.32
84	HV147	359627	4262191	-	-	3.00	0.97	1.03	9.28
85	HV148	359305	4262452	-	-	3.42	1.13	0.88	10.35
86	HV149	358526	4262190	-	-	3.27	1.75	0.57	6.11
87	HV150	358785	4262097	-	-	2.38	1.33	0.75	4.26
88	HV151	359042	4262228	-	-	2.28	0.96	1.04	5.42
89	HV152	359305	4261839	-	-	4.07	0.34	2.94	48.72
90	HV153	359794	4261347	-	-	7.80	0.64	1.56	95.06
91	HV154	360141	4261383	-	-	3.77	1.38	0.72	10.30
92	HV155	360022	4261024	-	-	3.56	1.21	0.83	10.47
93	HV156	360350	4262068	-	-	3.50	1.15	0.87	10.65
94	HV157	360629	4262112	-	-	3.85	1.13	0.88	13.12
95	HV158	360907	4261604	-	-	2.12	1.55	0.65	2.90
96	HV159	358203	4261701	-	-	3.75	1.02	0.98	13.79
97	HV160	360546	4262454	-	-	3.28	1.07	0.93	10.05
98	HV161	355429	4262838	-	-	3.11	1.45	0.69	6.67
99	HV163	358593	4262490	-	-	2.90	1.39	0.72	6.06
100	HV164	358947	4262543	-	-	3.12	0.62	1.62	15.77
101	HV165	359008	4262392	-	-	3.50	1.23	0.81	9.92
102	HV166	358020	4261797	-	-	4.14	1.28	0.78	13.37
103	HV167	359098	4261849	-	-	3.80	1.25	0.80	11.55
104	HV168	359023	4261925	-	-	3.70	1.28	0.78	10.68
105	HV169	359143	4261714	-	-	3.70	0.71	1.40	19.17
106	HV170	356829	4262573	-	-	4.21	0.68	1.47	26.05
107	HV171	359219	4262565	-	-	3.00	0.67	1.50	13.50
108	HV172	359336	4262541	-	-	2.90	1.23	0.81	6.81
109	HV173	259457	4262538	-	-	3.12	1.25	0.80	7.79
110	HV174	359479	4262442	-	-	3.20	1.30	0.77	7.88
111	HV175	359191	4262476	-	-	3.10	1.11	0.90	8.65
112	HV176	359095	4262479	-	-	3.00	0.71	1.40	12.60
113	HV177	358969	4262661	-	-	4.40	1.11	0.90	17.42
114	HV178	358876	4262621	-	-	3.96	1.28	0.78	12.23
115	HV179	359114	4262621	-	-	3.00	0.77	1.30	11.70
116	HV180	358845	4262300	-	-	3.00	0.83	1.20	10.80
117	HV181	358923	4262226	-	-	3.20	0.77	1.30	13.31
118	HV182	359390	4262792	-	-	3.40	0.63	1.60	18.50
119	HV183	359293	4262711	-	-	3.30	0.71	1.40	15.25
120	HV185	355647	4262924	-	-	2.04	9.09	0.11	0.46

cross-section, high period values were observed. It was seen that the building damage rate was increased in the same area (Fig. 6(b)).

It can be seen that the HVSR period values range from 0.11 s to 2 s when evaluating the predominant period. Areas nearest to Lake Van, western sites of the study area, and some areas in the city center have comparatively higher predominant period values (Fig. 4(a)). Higher period values in these areas indicate that they are composed of weak soil and have a thick soil layer. Period values decrease in the eastern, southern, and northern sites of the study area due to increasing topography and the presence of different types of rock units (Fig. 4(a)). Relatively higher HVSR peak values (amplitude) were observed in the western sites of the region (Fig. 4(b)). In the southern and eastern sites of the Van settlement area, the amplitude values decreased. In other words, it can be said that the fundamental period value is inversely proportional to the stability of the measured geological unit. When the regional geology and morphology are examined, these results are observed to be compatible with the geological structure. These results show that HVSR results are related to the soft sediments thickness and can be used for damage estimation.

4 Determination of seismic vulnerability index (K_g) with HVSR method

Earthquake waves have different amplitude and frequency or period contents. Earthquake waves cause stress on the structure and ground due to different periods in the contents. Overcoming the strain limit plays a significant role in the collapse of the structure. Nakamura (1997) suggested that the K_g value could be used to estimate both the weak points of soil and earthquake damage before a destructive earthquake. Surface shear

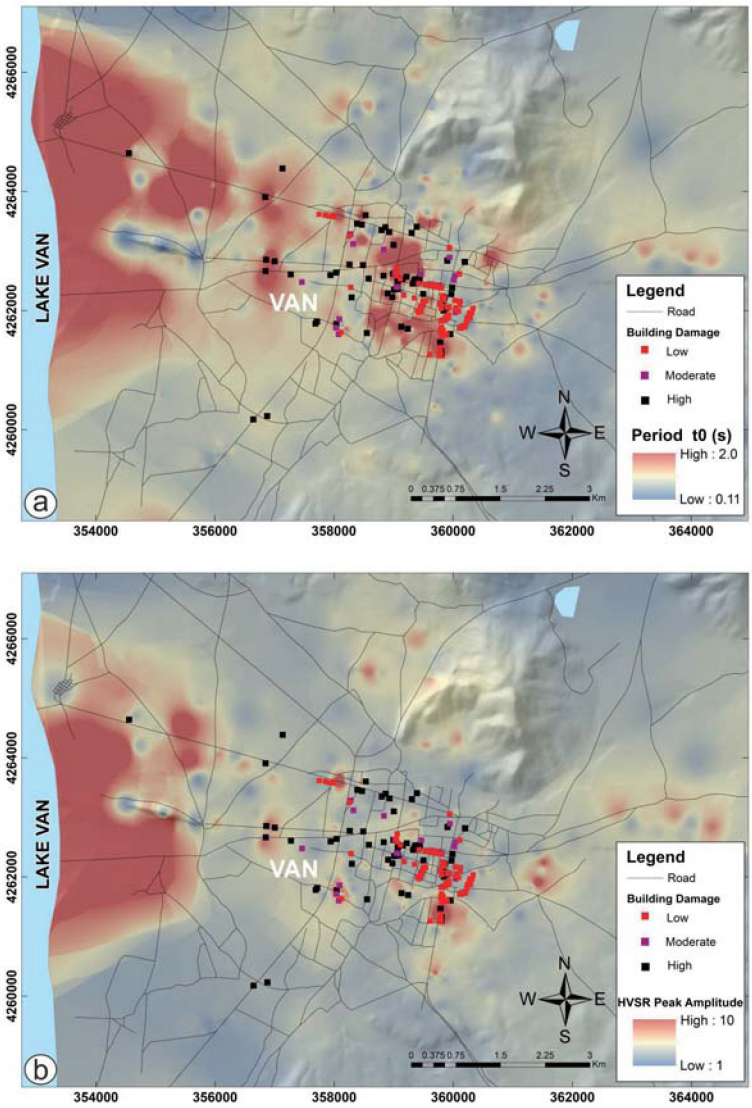

Fig. 4 (a) Predominant period and (b) HVSR amplitude maps of the study area

strain (γ) is also widely used in ground definition. Ishihara (1982) indicated that nonlinear behavior of the surface ground deformation from $\gamma \cong 10^{-3}$ goes into a plastic state, resulting in $\gamma > 10^{-2}$ which can lead to large deformation events such as landslide and collapse. Nakamura (1997) defined by focus on the strain in the K_g (Fig. 5).

The K_g value is a parameter depending on the dynamic properties of soil. With this parameter, it is possible to evaluate the vulnerability of a point-based site under strong ground motion. Since it is related to the natural vibration period and amplification factor, the parameter can be calculated for both soil and structure. Nakamura (1997, 2000) stated that the unit shear deformation on the ground surface due to an earthquake is related to the frequency and amplitude of the ground.

Nakamura (2000, 2008) suggested that the K_g value can be used to calculate the damage/strain of buildings and ground during a possible earthquake. Average shear strain (γ) value, as shown in Fig. 5 for surface ground, is calculated as follows:

$$\gamma = A_g \frac{d}{h} \tag{1}$$

where d is the seismic displacement of the basement, h is the layer thickness, and A_g is the factor of amplification (Fig. 5). Shear wave velocity values of bedrock and soil are V_b and V_s, respectively. The predominant frequency of the ground unit on engineering foundation is F_g (Nakamura, 2000, 2008):

$$F_g = \frac{V_b}{(4A_g\ h)} \tag{2}$$

For acceleration of basement a and displacement d as follows:

$$\begin{aligned} a &= w^2 d = (2\pi F_g)^2 d \\ d &= a/(2\pi F_g)^2 \end{aligned} \tag{3}$$

If shear deformation F_g and d are written in Eq. (1)

$$\begin{aligned} \gamma &= \frac{A_g\ \alpha_b}{(2\pi F_g)^2}\ 4A_g\ \frac{F_g}{C_b} \\ &= \frac{A_g^{\ 2}}{F_g}\frac{\alpha_b}{\pi^2 C_b} \\ &= c\ K_g \alpha_b \end{aligned} \tag{4}$$

where

$$c = \frac{1}{\pi^2\ v_b}\ K_g = \frac{A_g^{\ 2}}{F_g} \tag{5}$$

c is expected to be almost the same in large areas due to the shear wave velocity of the basement. In this case, the K_g value remains unique to the working point and is referred to as the "Seismic vulnerability Index". Effective shear strain described by % e of Eq. (4) becomes approximately equal to the K_g and α_b, under the assumptions of e = 60% and V_b = 600 m/s.

Weak or strong areas can be determined with the K_g value for the research sites and the damage possibility can be calculated. This value defines the level of surface layer vulnerability to deformation during earthquakes (Nakamura, 1997, 2000, 2008). Nakamura (1997) showed that the K_g value at the sites where soil deformation is much higher than 20 and the K_g value is very small in undamaged areas.

In this study, the K_g value was calculated by using microtremor measurements (Fig. 6). The limit values of K_g as follows:

$K_g \leq 3$ Low

$3 < K_g \leq 5$ Moderate

$5 < K_g \leq 10$ High

$K_g \geq 10$ Very high

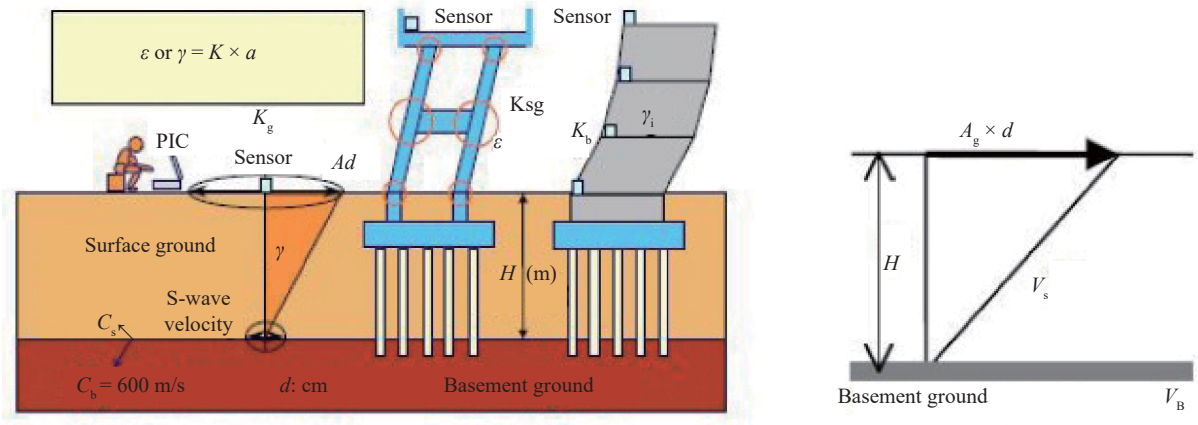

Fig. 5 Simply shear deformation of surface ground (modified from Nakamura, 2008)

It can be seen that the K_g values range from 0.29 to more than 100 when evaluating the K_g map (Fig. 6(a)). Areas nearest to Lake Van, western sites of the area, and some areas in the city center have relatively higher K_g values (Fig. 6(a)). Higher K_g and period values in the same areas indicate that they are composed of weak soil. In the southern and eastern parts of the Van settlement area, the K_g values decreased (Fig. 6(a)). The results show that the sites with $K_g > 10$ is where possible structural damage can occur.

When the buildings damaged by the 2011 Van earthquake ($M_w = 7.1$) were examined, it was observed that the damage ratio of the buildings may be related to the K_g and period values (Fig. 6(b)). There is a high correlation, approximately 80 percent, between the damage rate map based on the damaged building data (Fig. 6(b)) and the K_g values (Fig. 6(a)). As the values of soil and structure vulnerability indices increase, the degree of damage will also increase. In order to determine the damage more precisely, it is necessary to determine both soil and structures vulnerability indices.

Figure 7 illustrates the average shear wave velocity up to a depth of 30 m (V_{s30}) and NEHRP soil classification map of the study area. These maps were prepared using geological boreholes and geophysical applications (Akkaya *et al*., 2018b). The V_{s30} values range from 200 to 1250 m/s (Fig. 7(a), Table 1). In general, low velocity values were obtained throughout the study area except for rock units. According to the NEHRP (1997) soil classification criteria based on V_{s30} values, the study area was mostly of NEHRP classes D and C (Fig. 7(b), Table 1). These areas have relatively higher K_g values ($K_g >$ 10), while other types of soil generally have K_g values that are smaller than 10. In addition, V_{s30} values in areas with weak soil and high K_g values were found to be < 250 m/s (Fig. 7).

In addition, the possible correlations between the data obtained in the study were examined. Relationships

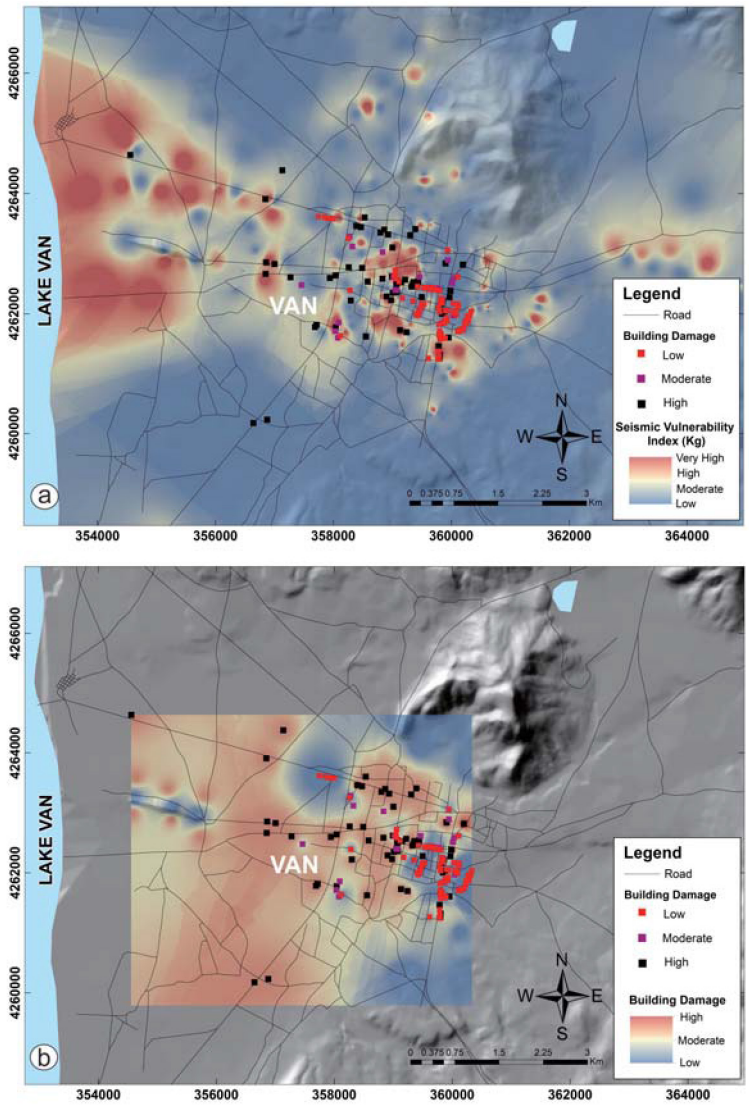

Fig. 6 (a) K_g values and (b) building damage ratio map of the study area

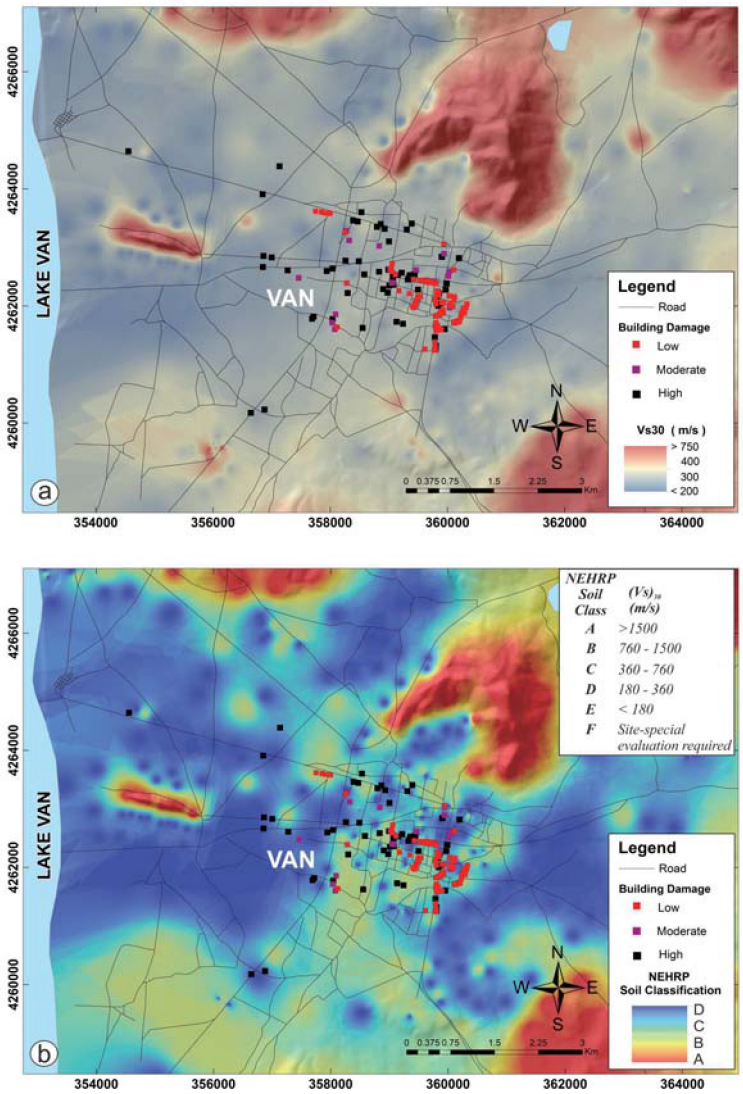

Fig. 7 (a) V_{s30} and (b) NEHRP soil classification map of the study area

are calculated as follows;

$$V_{s30} = 192.69\, t_0^{-0.765} \quad R^2 = 0.57 \tag{6}$$

$$V_{s30} = 568.74\, K_g^{-0.412} \quad R^2 = 0.84 \tag{7}$$

It can be seen that there is a good correlation between the V_{s30} values obtained for the study area and the K_g and period (t_0) values. In both data sets, the data fit to the exponential trend was determined (Fig. 8). A linear regression was applied to both data sets, and it was obtained with a high correlation coefficient. As a result, it can be said that there is an inverse relation between V_{s30} and both period and K_g values.

5 Building damage assessments

Although some buildings in the region survived with minor and moderate damage, they do not necessarily have adequate strength or are safe in the event of future earthquakes. For this reason, their seismic performance should be determined to prevent losses in future seismic events. Therefore, some of the buildings examined in the study area have already been evaluated in terms of structural damage.

The reasons for the collapse and severe damage to buildings generally depends on several parameters such as the soil conditions, number of stories, low concrete grade or concrete strength, lack of reinforcement detailing, weight of the building, inadequate workmanship, irregularities, and so on (Saatcioglu *et al*., 2001; Sucuoğlu and Yazgan, 2003; Bayraktar *et al*., 2014; Akansel *et al*., 2014; Erdil, 2017; Erdil and Ceylan, 2019a-b). Each parameter may have a strong influence on damage in some cases.

In this study, 188 of the buildings in Van with varying structural properties (Table 2) were investigated. Among these, 94 experienced minor or no damage and

26 were moderately damaged. 58 buildings had heavy damage and 10 buildings collapsed. The relationship between the number floors and structural irregularities of the buildings are shown in Fig. 9. As illustrated in the figure, the investigated buildings had two to nine stories, with the majority having four and seven stories. Note that there is no precise relationship between the number of stories and the damage state. However, the building damage ratio starts to increase for buildings with more than four stories.

The irregularities due to horizontal and vertical structural elements are not capable of regularly transferring earthquake loads and are among the reasons for damage to the buildings. The irregularity parameter information in the buildings is shown in Table 2 and Fig. 10. Table 2 summaries the following information about the investigated buildings.

28% of the 16 buildings with short column irregularity in 9% were heavily damaged or destroyed

57% of the 96 buildings with soft story irregularity in 51% were heavily damaged or destroyed

64% of the 114 buildings with heavy overhang irregularity in 61% were heavily damaged or destroyed

54% of the 41 buildings with frame irregularity in 22% were heavily damaged or destroyed

In addition to building irregularities, number of stories, concrete strength, ground floor area, and the area of the total vertical (column and shear wall)

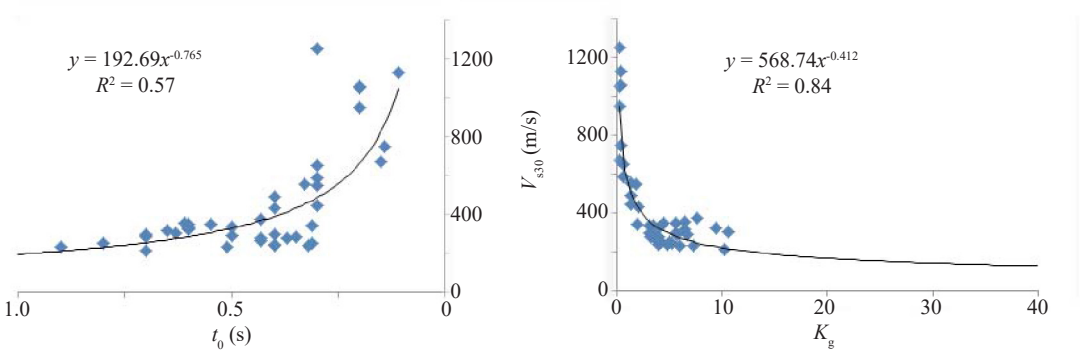

Fig. 8 Correlation between (a) V_{s30} and predominant period and (b) V_{s30} and K_g values

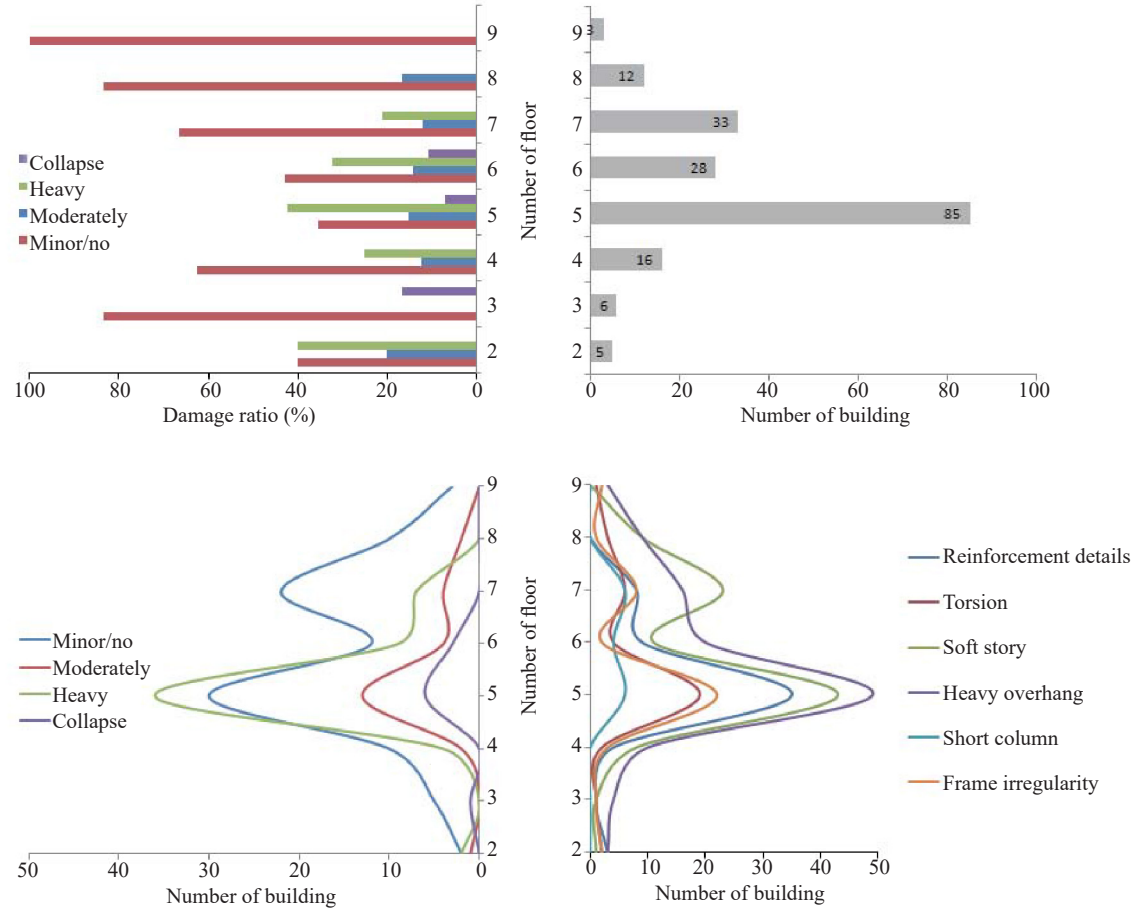

Fig. 9 Investigation of the damage ratio and irregularities of buildings in the study area

Table 2 Irregularities and damage states of the investigated buildings

Number of floor	Number of building	Damage ratio								Building irregularities											
		Minor/no		Moderately		Heavy		Collapse		Reinforcement details		Torsion		Soft story		Heavy overhang		Short column		Frame irregularity	
		#	%	#	%	#	%	#	%	#	%	#	%	#	%	#	%	#	%	#	%
2	5	2	40	1	20	2	40	0	0	3	60	2	40	1	20	3	60	0	0	2	40
3	6	5	83	0	0	0	0	1	17	1	17	1	17	1	17	4	67	0	0	1	17
4	16	10	63	2	13	4	25	0	0	4	25	2	13	8	50	10	63	0	0	3	19
5	85	30	35	13	15	36	42	6	7	35	41	19	22	43	51	49	58	6	7	22	26
6	28	12	43	4	14	9	32	3	11	9	32	4	14	11	39	20	71	4	14	2	7
7	33	22	67	4	12	7	21	0	0	8	24	6	18	23	70	16	48	6	18	8	24
8	12	10	83	2	17	0	0	0	0	0	0	3	25	9	75	9	75	0	0	1	8
9	3	3	100	0	0	0	0	0	0	0	0	1	33	0	0	3	100	0	0	2	67
Total	**188**	**94**		**26**		**58**		**10**		**60**		**38**		**96**		**114**		**16**		**41**	
%		**50**		**14**		**31**		**5**		**32**		**20**		**51**		**61**		**9**		**22**	

Fig. 10 Building damage caused by building irregularities after 2011 Van earthquakes (a: short column; b: soft story; c: concrete strength; d: heavy overhang)

load carrying members played an important role in reducing the damage state in the investigated buildings. However, these properties may not be reasonable and may not represent solely the effects of the earthquake resistance of a building. Therefore, instead of using a single parameter to determine the seismic vulnerability of a building, several interrelated parameters should be interactively evaluated together.

6 Conclusion

The aim of this study was to investigate the effect of soil and building properties on structural damage in the Van province and surrounding areas, which were severely damaged following a major earthquake in 2011. The analysis is based on the results of data processing and interpretation of the parameters of

amplification, predominant frequency and K_g value. Since the earthquake waves have different amplitude and frequency or period contents, they cause stress on the structure and ground. Overcoming the strain limit plays a crucial role in the collapse of a structure. The K_g value can be used to estimate both the weak points of soil and earthquake damage before a destructive earthquake. The K_g value depends on the dynamic properties of the soil obtained from the HVSR microtremor method.

HVSR microtremor measurements were recorded at more than 200 locations throughout the Van region to generate the predominant period, amplification, and K_g map. HVSR period values range from 0.11 s to 2 s and HVSR measurements showed that the western parts of the study area, especially those nearest to Lake Van, and some areas in the city center had higher predominant period values (0.6–1.5 s). Higher amplitudes were observed in the same areas (3–8). Higher period and amplitude values in the same areas indicate that they are composed of weak soil. High period values (> 1 s) are very dangerous, especially for buildings with many floors due to the possibility of resonance. Period values were lower in the southern, eastern, and northern parts of the region (0.11–0.3 s), where rock and hard soil are located. In the eastern and southern sites of the Van settlement area, the amplitude values decreased (1–3). Low period and amplitude values in the same areas indicate that they are composed of hard soil and rock. Low and intermediate predominant period values could result in severe damage to both tall and short floor buildings in the city.

All the results showed good correlation between the soil type and HVSR microtremor results measured at various locations in the study area. The alluvial sites had high predominant periods and low V_{s30} values, which is consistent with thick soil layers. On the other hand, low thickness sediments and rocks had low predominant periods and high V_{s30} values, and the building damage rate was higher in this area. These observations show that HVSR results are related to the soft sediments thickness and can be used for damage estimation.

The K_g value was evaluated by using the predominant frequency and amplification, which were used to estimate the earthquake hazard potential of the region. The K_g values ranged from 0.29 to more than 100 when evaluating the K_g distribution map. After the map was generated, it was seen that the hazard potential and seismic vulnerability index was high at the sites nearest to Lake Van and at the densely populated city center. In the southern and eastern sites of the Van settlement area, the K_g values decreased. The results show that the sites with $K_g > 10$ are vulnerable to structural damage.

The V_{s30} and NEHRP soil classification map of the study area illustrate that low velocity values (< 250 m/s) were obtained throughout the area except for rock. In addition, the area was mostly classified as D and C types of soil based on the NEHRP classification criteria. In addition, there was good correlation between the V_{s30} values obtained for the study area and the K_g and period values. In both data sets, the data fit to the exponential trend was determined with a high correlation coefficient.

$$V_{s30} = 192.69\, t_0^{-0.765} \quad R^2 = 0.57$$

$$V_{s30} = 568.74\, K_g^{-0.412} \quad R^2 = 0.84$$

The reasons for the collapses and severely damaged buildings are generally depends on several parameters, such as the soil conditions, number of stories, low concrete grade or concrete strength, lack in reinforcement detailing, weight of the building, inadequate workmanship, irregularities. Building irregularities are the one of causes of earthquake damage. As seen in the investigated buildings, the 16 buildings with short column irregularity in 9%, the 96 buildings with soft story irregularity in 51%, the 114 buildings with heavy overhang irregularity in 61%, and the 41 buildings with frame irregularity in 22% were heavily damaged or destroyed in the area. In addition to these irregularities, the number of stories, concrete strength, ground floor area, and the area of the total vertical load carrying members played an important role in reducing the damage state.

Damage information was placed on the period and K_g map and it was seen that there could be a correlation between the damage and the K_g. There is a high correlation, approximately 80 percent, between the damage rate map based on the damaged building data and the K_g values. It is likely that this rate will increase if more building data is obtained. As the values of soil and structure vulnerability indices increase, the degree of damage will also increase. From the results of this study and the site observations after the 2011 Van earthquakes, structural damage is not only structure-dependent but is also related to the dynamic behavior of soil layers and local soil conditions.

The city of Van and the surrounding area, located in the eastern part of the Lake Van basin, is on water-saturated alluvial soils consisting of lake and stream sediments. Such soils are greatly affected by large earthquakes, and repeated earthquake loads cause deformation. It is part of a very active seismic area in eastern Anatolia that includes a wide range of geologic features that has a high potential to produce large earthquakes. A major earthquake might cause additional damage to buildings in this region.

This study shows that building properties and local soil conditions directly affect the damage level of structures after a destructive earthquake. Therefore, instead of using a single parameter to determine the seismic performance of a building, several interrelated parameters should be interactively evaluated together.

Acknowledgement

The Scientific Research Projects Office of

Van Yüzüncü Yıl University Project Number 2015-MIM-B259 financially supported this study. The author thanks Assist. Prof. Dr. Barış Erdil for his support during the compilation and evaluation of building damage data stages presented herein. The author also thanks the reviewers for their constructive comments, which enhanced the quality of the paper.

References

AFAD, *Disaster & Emergency Management Authority of Turkey*, Available: https://www.afad.gov.tr/.

Akansel V, Ameri G, Askan A, Caner A, Erdil B, Kale Ö and Okuyucu D (2014), "The 23 October 2011 M_w = 7.0 Van (Eastern Turkey) Earthquake: Interpretations of Recorded Strong Ground Motions and Post-Earthquake Conditions of Nearby Structures," *Earthquake Spectra*, **30**(2): 657–682.

Akın Ö and Sayıl N (2016), "Site Characterization Using Surface Wave Methods in the Arsin-Trabzon Province, NE Turkey," *Environ Earth Sci.*, **75**: 72, DOI 10.1007/s12665-015-4840-6.

Akkaya İ (2015), "The Application of HVSR Microtremor Survey Method in Yüksekova (Hakkari) Region, Eastern Turkey," *Journal of African Earth Sciences*, **109**: 87–95.

Akkaya İ, Özvan A, Tapan M and Şengül MA (2015), "Determining the Site Effects of 23 October 2011 Earthquake (Van province, Turkey) on the Rural Areas Using HVSR Microtremor Method," *Journal of Earth System Science*, **124**(7): 1429–1443.

Akkaya İ, Özvan A, Akın M, Akın MK, and Övün U (2017), "Kayma Dalgası Hızı (Vs) Kullanılarak Erciş (Van) Yerleşim Alanının Sıvılaşma Potansiyelinin Değerlendirilmesi," *Çukurova Üniversitesi Mühendislik Mimarlık Fakültesi Dergisi*, **32**(3): 55–68. (in Turkish)

Akkaya İ, Özvan A, Akın M, Akın MK, and Övün U (2018a), "Comparison of SPT and Vs-Based Liquefaction Analyses: A Case Study in Erciş (Van, Turkey)," *Acta Geophysica*, **66**: 21–38. https://doi.org/10.1007/s11600-017-0103-0.

Akkaya İ, Özvan A and Tapan M (2018b), "Determination of Dynamic Characteristics of Quaternary Soils and Local Soil Conditions in Van and Surroundings by Geophysical Methods," *The Scientific Research Projects Office of Van Yuzuncu Yil University Project Number 2015-MIM-B259*, 138 pages.

Akkaya İ and Özvan A (2019), "Site Characterization in the Van Settlement (Eastern Turkey) Using Surface Waves and HVSR Microtremor Methods," *Journal of Applied Geophysics*, **160**: 157–170.

Ambraseys NN and Finkel CF (1995), *The Seismicity of Turkey and Adjacent Areas: A Historical Review, 1500–1800*, İstanbul: Eren publishing & booktrade.

Ambraseys NN (2001), "Reassessment of Earthquakes 1900–1999 in the Eastern Mediterranean and Middle East.," *Geophys. J. Int.*, **145**: 471–485.

Ansal A (1999a), "Strong Ground Motions and Site Amplification. Theme Lecture," *2nd Int. Conf. on Earthquake Geotechnical Engineering*, **3**: 879–894, Ed.P.S.Pinto, Balkema, Rotterdam.

Ansal A (1999b), "The Cyclic Behavior of Soils and Effects of Geotechnical Factors During 17 August 1999 Kocaeli Earthquake," *Earthquake Hazard and Risk in the Mediterranean Region*, Nicosia, **1**: 89–104.

Bard PY (1998), "Microtremor Measurements: A Tool for Site Effect Estimation," *Proceedings of 2nd International Symposium on the Effect of Surface Geology on Seismic Motion*, 1-3 Dec, Yokohama, Japan, **3**: 1251–1279.

Bayraktar A, Altunisik A, Türker T, Karadeniz H, Erdogdu S, Angin Z and Özsahin T (2014), "Structural Performance Evaluation of 90 RC Buildings Collapsed during the 2011 Van, Turkey, Earthquakes," *J. Perform. Constr. Facil.*, 10.1061/(ASCE)CF.1943-5509.0000524, 04014177.

Birgören G, Ozel O and Siyahi B (2009), "Bedrock Depth Mapping of the Coast South of Istanbul: Comparison of Analytical and Experimental Analyses," *Turkish Journal of Earth Sciences*, **18**: 315–329.

Bonnefoy-Claudet S, Cotton F and Bard PY (2006), "The Nature of Noise Wavefield and Its Applications for Site Effects Studies: A Literature Review," *Earth-Science Reviews*, **79**: 205–227.

Bozkurt E (2001), "Neotectonics of Turkey-a Synthesis," *Geodinamica Acta*, **14**: 3–30.

Claprood M, Asten M and Kristek J (2012), "Combining HVSR Microtremor Observations with the SPAC Method for Site Resonance Study of the Tamar Valley in Launceston (Tasmania, Australia)," *Geophysical Journal International*, **191**: 765–780.

Cukur D, Krastel S, Tomonaga Y, Schmincke H-U, Sumita M, Meydan AF, Cagatay MN, Toker M, Kim S-P, Kong G-S and Horozal S (2016), "Structural Characteristics of the Lake Van Basin, Eastern Turkey, from High-Resolution Seismic Reflection Profiles and Multibeam Echosounder Data: Geologic and Tectonic Implications," *Int. J. Earth Sci.* (*Geol Rundsch*), http://dx.doi.org/10.1007/s00531-016-1312-5.

Delgado J, Lopez Casado C, Giner J, Estevez A, Cuenca A and Molina S (2000), "Microtremors as a Geophysical Exploration Tool: Applications and Limitations," *Pure and Applied Geophysics*, **157**: 1445–1462.

Dikmen Ü and Mirzaoğlu M (2005), "The Seismic Microzonation Map of Yenisehir-Bursa, NW of Turkey by Means of Ambient Noise Measurements," *Balkan Geophysical Society*, **8**(2): 53–62.

Dindar H, Dimililer K, Özdağ ÖC, Atalar C, Akgün M and Özyankı A (2017), "Vulnerability Index Assessment Using Neural Networks (VIANN): A Case Study of Nicosia, Cyprus," *ISPRS Annals of the Photogrammetry,*

Remote Sensing and Spatial Information Sciences, Volume IV-4/W4, 2017 4th International GeoAdvances Workshop, 14–15 October 2017, Safranbolu, Karabuk, Turkey.

Emre Ö, Duman TY, Özalp S, Elmacı H, Olgun Ş and Şaroğlu F (2013), "1/1.250.000 Ölçekli Türkiye Diri Fay Haritası," *Maden Tetkik ve Arama Genel Müdürlüğü Özel Yayınlar Serisi*, Ankara, Türkiye. (in Turkish)

Erdil B (2017), "Why RC Buildings Failed in the 2011 Van, Turkey, Earthquakes: Construction Versus Design Practices," *Journal of Performance of Constructed Facilities*, **31**(3): doi.org/10.1061/(ASCE)CF.1943-5509.0000980.

Erdil B and Ceylan H (2019a), "MVP Interaction Based Seismic Vulnerability Assessment of RC Buildings," *Gradevinar*, **71**: 489–503.

Erdil B and Ceylan H (2019b), "A Detailed Comparison of Preliminary Seismic Vulnerability Assessment Methods for RC Buildings," *Iranian Journal of Science and Technology-Transactions of Civil Engineering*, **43**:711–725.

Eskişar T, Özyalın Ş, Kuruoğlu M and Yılmaz HR (2013), "Microtremor Measurements in the Northern Coast of İzmir Bay, Turkey to Evaluate Site-Specific Characteristics and Fundamental Periods by H/V Spectral Ratio Method," *J. Earth Syst. Sci.*, **122**(1): 123–136.

Fah D, Kind F and Giardini D (2001), "A Theoretical Investigation of Average H/V Ratios," *Geophysical Journal International*, **145**: 535–549.

Field EH and Jacob KH (1993), "The Theoretical Response of Sedimentary Layers to Ambient Seismic Noise," *Geophys Res Lett*, **20-24**: 2925–2928.

Field EH and Jacob KH (1995), "A Comparison and Test of Various Site-Response Estimation Techniques, Including Three That are not Reference-Site Dependent," *Bull. Seismol. Soc. Am.*, **85**(4): 1127–1143.

Gallipoli MR, Mucciarelli M, Gallicchio S, Tropeano M and Lizza C (2004), "Horizontal to Vertical Spectral Ratio (HVSR) Measurements in the Area Damaged by the 2002 Molise, Italy, Earthquake," *Earthq Spectra*, **20**(S1): S81–S93.

Gallipoli MR and Mucciarelli M (2009), "Comparison of Site Classification from VS30, VS10, and HVSR in Italy," *Bull Seismol Soc Am*, **99**: 340–351.

GEOPSY (1997), *Geophysical Signal Database for Noise Array Processing*, www.geopsy.org, Accessed June 2015.

Gitterman Y, Zaslavsky Y, Shapira A and Shtivelman V (1996), "Empirical Site Response Evaluations: Case Studies in Israel," *Soil Dynamics Earthquake Engineering*, **15**: 447–463.

Ishihara K (1982), "Evaluation of Soil Properties for Use in Earthquake Response Analysis," *Proc. International Symp. On Num. Model in Geomechanics*, 237–259.

Koçyiğit A, Yilmaz A, Adamia S and Kulashvili S (2001), "Neotectonics of East Anatolian Plateau (Turkey) and Lesser Caucasus: Implication for Transition from Thrusting to Strike-Slip Faulting," *Geodinamica Acta*, **14**: 177–195.

Koçyiğit A (2013), "New Field and Seismic Data about the Intraplate Strike-Slip Deformation in Van Region, East Anatolian Plateau, E.Turkey," *Journal of Asian Eart Sciences*, **62**: 586–605.

KOERI (2011), "Probabilistic Assessment of the Seismic Hazard for the Lake Van basin, October, 23 2011," www.koeri.boun.edu.tr, Accessed 23 Dec 2012.

KOERI, *Bogazici University Kandilli Observatory and Earthquake Research Institute Regional Earthquake-Tsunami Monitoring Center* (*KOERI*) *website*, Available: http://www.koeri.boun.edu.tr/sismo/2/en/.

Konno K and Ohmachi T (1998), "Ground-Motion Characteristics Estimated from Spectral Ratio Between Horizontal and Vertical Components of Microtremor," *Bulletin of the Seismological Society of America*, **88**: 228–241.

Lachet C and Bard PY (1994), "Numerical and Theoretical Investigations on the Possibilities and Limitations of Nakamura's Technique," *Journal of Physics of the Earth*, **42**: 377–397.

Lermo J and Chavez-Garcia FJ (1993), "Site Effect Evaluation Using Spectral Ratios with Only One Station," *Bulletin of the Seismological Society of America*, **83**: 1574–1594.

Lermo J and Chavez-Garcia FJ (1994), "Are Microtremors Useful in Site Response Evaluation?" *Bulletin of the Seismological Society of America*, **84**: 1350–1364.

Livaoğlu H, Irmak TS and Güven IT (2017), "Seismic Vulnerability Indices of Ground for Değirmendere (Kocaeli Province, Turkey)," *Bull Eng Geol Environ*, DOI 10.1007/s10064-017-1102-8.

Mucciarelli M (1998), "Reliability and Applicability of Nakamura's Technique Using Microtremors: An Experimental Approach," *Journal of Earthquake Engineering*, **2**: 1–14.

Nakamura Y (1989), "A Method for Dynamic Characteristics Estimation of Subsurface Using Microtremor on the Ground Surface," *QR of RTRI*, **30**: 25–33.

Nakamura Y (1997), *Seismic Vulnerability Indices for Ground and Structures Using Microtremor*, World Congress on Railway Research, Florence.

Nakamura Y (2000), "Clear Identification of the Fundamental Idea of Nakamura's Technique and Its Applications," *In: 12th World Conference on Earthquake Engineering*, New Zealand (CD-ROM), Paper No. 2656.

Nakamura Y (2008), "On the H/V Spectrum," *The 14th World Conference on Earthquake Engineering*, Beijing, China.

Nath SK, Adhikari MD, Devaraj N and Maiti SK (2015), "Seismic Vulnerability and Risk Assessment of Kolkata City, India," *Nat. Hazards Earth Syst. Sci.*, **15**: 1103–1121.

NEHRP (1997), *Recommended Provisions For Seismic Regulations For New Buildings and Other Structures*, *FEMA-303*, Prepared by the Building Seismic Safety Council for the Federal Emergency Management Agency, Washington, DC.

Okada H (2003), *The Microtremor Survey Method*, Geophysical Monograph, No. 12, Society of Exploration Geophysicists, Tulsa.

Özvan A, Akkaya İ, Tapan M and Şengül MA (2005), "Van Yerleşkesinin Deprem Tehlikesi ve Olası bir Depremin Sonuçları," *Deprem Sempozyumu Kocaeli 2005*, 23–25 Mart 2005, Kocaeli. (in Turkish)

Özalaybey S, Zor E, Ergintav S and Tapırdamaz MC (2011), "Investigation of 3-D Basin Structures in the İzmit Bay Area (Turkey) by Singlestation Microtremor and Gravimetric Methods," *Geophysical Journal International*, **186**: 883–894.

Pamuk E, Özdağ CÖ, Tucçel A, Özyalın Ş and Akgün M (2017a), "Local Site Effects Evaluation for Aliağa/İzmir Using HVSR (Nakamura technique) and MASW methods," *Nat Hazards*, DOI 10.1007/s11069-017-3077-y.

Pamuk E, Akgün M, Özdağ ÖC and Gönenç T (2017b), "2D Soil and Engineering-Seismic Bedrock Modeling of Eastern Part of Izmir Inner Bay/Turkey," *Journal of Applied Geophysics*, **137**: 104–117.

Pamuk E, Özdağ ÖC, Özyalın Ş and Akgün M (2017c), "Soil Characterization of Tınaztepe Region (İzmir/Turkey) Using Surface Wave Methods and Nakamura (HVSR) Technique," *Earthquake Engineering and Engineering Vibration*, **16**(2): 447–458.

Paudyal YR, Yatabe R, Bhandary NP, and Dahal RK (2012), "A Study of Local Amplification Effect of Soil Layers on Ground Motion in the Kathmandu Valley Using Microtremor Analysis," *Earthquake Engineering and Engineering Vibration*, **11**: 257–268.

Saatcioglu M, Mitchell D, Tinawi R, Gardner NJ, Gillies AG, Ghobarah A, Anderson DL and Lau D (2001), "The August 17, 1999, Kocaeli (Turkey) Earthquake Damage to Structures," *Canadian Journal of Civil Engineering*, **28**(4): 715–737.

Şaroğlu F and Yılmaz Y (1986), "Doğu Anadolu'da Neotektonik Dönemdeki Jeolojik Evrim ve Havza Modelleri," *MTA Genel Müdürlüğü, Jeoloji Etütleri Dairesi*, Ankara. (in Turkish)

Selçuk AS (2016), "Evaluation of the Relative Tectonic Activity in the Eastern Lake Van basin, East Turkey," *Geomorphology*, **270**: 9-21.

Şengör AMC and Kidd WSF (1979), "Post-Collisional Tectonics of the Turkish–Iranian Plateau and a Comparison with Tibet," *Tectonophys*, **55**: 361–376.

SESAME (2004), *Guidelines for the Implementation of the H/V Spectral Ratio Technique on Ambient Vibrations: Measurements, Processing and Interpretation SESAME European Research Project* P12-Deliverable. D23.12 ftp://ftp.geo.uib.no/pub/seismo/Software/Sesame/Userguidelines/Sesame-HV-UserGuide lines.doc.

Silahtar A, Budakoğlu E, Horasan G, Yıldırım E, Küyük HS, Yavuz E and Çaka D (2016), "Investigation of Site Properties in Adapazarı, Turkey, Using Microtremors and Surface Waves," *Environ Earth Sci*, **75**: 1354, DOI 10.1007/s12665-016-6151-y.

Soysal H, Sipahioğlu S, Kolçak D and Altınok Y (1981), "Türkiye ve Çevresinin Tarihsel Deprem Kataloğu (2100 B.C.–1900 A.D.)," *TÜBİTAK raporu*, No. TBAG-341. (in Turkish)

Sucuoglu H and Yazgan U (2003), "Simple Survey Procedures For Seismic Risk Assessment İn Urban Building Stocks," Chap. 6, *Seismic Assessment and Rehabilitation of Existing Buildings, Earth and Environmental Sciences* (Editör: S. T. Wasti, G. Özcebe), London: Kluwer Academic Publishers, **29**: 97–118.

Tan O, Tapırdamaz MC and Yörük A (2008), "The Earthquakes Catalogues for Turkey," *Turkish Journal of Earth Science*, **17**: 405–418.

Theodulidis N, Bard PY, Archuleta R and Bouchon M (1996), "Horizontal-To-Vertical Spectral Ratio and Geological Conditions: the Case of Garner Valley Downhole in Southern California," *Bulletin of the Seismological Society of America*, **68**: 767–779.

Toker M, Şengör A, Demirel-Schlueter F, Demirbağ E, Çukur D, İmren C *et al*. (2017), "The Structural Elements and Tectonics of the Lake Van basin (Eastern Anatolia) from Multi-Channel Seismic Reflection Profiles," *Journal of African Earth Sciences*, **129**: 165–178.

Tün M, Pekkan E, Özel O and Güney Y (2016), "An Investigation into the Bedrock Depth in the Eskisehir Quaternary Basin (Turkey) Using the Microtremor Method," *Geophys. J. Int.*, **207**: 589–607.

Utkucu M (2013), "23 October 2011 Van, Eastern Anatolia, Earthquake (M_W 7.1) and Seismotectonics of Lake Van Area," *Journal of Seismology*, **17**: 783–805.